

Combined Application of Partition Clustering Classification and Gerchberg-Papoulis Optimization Algorithm for Spherical Near Field Antenna Measurements

Fangyun Peng¹, Yuchen Ma², Yuxin Ren², Bo Liu¹, Xiaobo Liu¹, Zhengpeng Wang³,
Lei Zhao⁴, Xiaoming Chen¹, and Zhiqin Wang²

¹School of Information and Communications Engineering
Xi'an Jiaotong University, Xi'an, 710049, China
pfy2014111731@stu.xjtu.edu.cn, liuboright@stu.xjtu.edu.cn, xiaoming.chen@mail.xjtu.edu.cn

²China Academy of Information and Communications Technology
Beijing, 100191, China
mayuchen@caict.ac.cn, renyuxin@caict.ac.cn, wangzhiqin@caict.ac.cn (author for correspondence)

³School of Electronic and Information Engineering
Beihang University, Beijing, 100191, China
wangzp@buaa.edu.cn

⁴School of Information and Control Engineering
China University of Mining and Technology, Xuzhou, 100083, China
leizhao@cumt.edu.cn

Abstract – An adaptive sampling and optimized extrapolation scheme for spherical near-field antenna testing is proposed. The method relies on the partition clustering classification algorithm and Voronoi classification to divide a small amount of initial data into subclasses and cells. The sampling density and rates of variation between adjacent sampling points are used as an overall metric function to evaluate the sampling dynamics at each location. Appropriate interpolation is performed in the highly dynamic region to increase the effective data in the near-field samples. The Gerchberg-Papoulis algorithm extrapolates the unnecessary interpolation region to improve the near-field sampling accuracy. This method uses a small amount of initial near-field sampled data for near-far field conversion to achieve the same precision as uniform oversampling. The feasibility and stability of the algorithm are proved from the actual measurement results.

Index Terms – adaptive sampling, cluster classification algorithm, extrapolation, spherical near-field testing.

I. INTRODUCTION

Compared with plane and cylindrical near-field testing, spherical near field testing (SNFT) scans the entire 3D near-field spherical information of the antenna under

test (AUT) with a uniform sampling interval through a single probe or multiple probes, and can obtain the complete information of the AUT in the entire 3D space. Spherical near-field to far-field (NF-FF) transformation techniques have been widely used to overcome the impossibility or impracticality of measuring antenna radiation patterns in the far field. The core of the SNFT is to use the characteristic that the spherical wave expansion coefficient remains unchanged in the near field (NF) and the far field (FF) to perform the spherical near-far field conversion [1–7]. Recently, the SNFT transformation technique has been applied to loaded/unloaded reverberation chambers for antenna pattern reconstruction [8, 9]. Nevertheless, calculation of spherical wave expansion coefficients for NF data with incomplete or large errors will cause large deviations.

There have been different solutions to the problem of truncation error and to demonstrate the reliability of the method in small truncation regions [10–16]. The authors in [10] proposed an iterative extrapolation-based machine learning algorithm to extend the calculation of the far field to a more accurate region, which employed an analysis of variance test to check the overall feasibility of the regression model. The authors in [11] used the Gerchberg-Papoulis (GP) iterative algorithm to extrapolate the part outside the truncation region. The NF sampling points were extended using a Slepian sequence

that is specially constructed to be orthogonal over a given truncated sweep circle, achieving more accurate results than the classical near-far-field transformation [12]. [13] adopted the truncation error in the measurement of the planar near-field aperture antenna by the alternate orthogonal projection method.

The large number of sampling points results in a long measurement time, which requires more flexibility in the sampling scheme. Measurements on the coarse grid were interpolated onto the finer grid using an optimal sampling interpolation (OSI) method to determine measurements for efficient recovery of non-uniform NF samples [17–18]. The compressed sensing (CS) method determines the minimum number of samples for near-field sparse recovery, which allows reducing the number of measurements for all antennas while maintaining accuracy [19–20]. However, the sparse level of NF sampled data and the prior information of the system had a great impact on the test results and are not suitable for all antenna tests. Based on measurements with helical scans, the authors in [21] investigated the application of non-uniform fast Fourier transforms in SNFT. A recently proposed method based on recursive partitioning in a multi-level subdomain hierarchy of radiating surfaces is applied to arbitrary surface measurements [22]. The authors in [23–25] described the adaptive method to reduce the measurement burden spherical near-field measurements. The fast irregular antenna field transformation algorithm (FIAFTA) was used to post-process the near field collected on an irregular grid [26] and the source reconstruction method was used to calculate the equivalent current on the surface of the ellipsoid containing the AUT [23]. These techniques require more time than fast Fourier near-far field transform methods.

In this paper, a spherical near-field sampling optimization method based on partition clustering classification and GP joint optimization is proposed. Starting from a small amount of sampled data, the clustering method is used to quantify the dynamic changes of the AUT NF electric field. There is a trade-off between sampling density and variation between adjacent sampling points according to different criteria. The new data is interpolated in the high dynamic change area of the field to improve the accuracy of the near-field sampling data and the GP iterative algorithm extrapolates the data to the unnecessary interpolation area to reduce the truncation error.

The structure of the paper is as follows. Section II introduces the theory of spherical wave expansion and the optimization scheme of spherical near-field sampling. Measurement results are presented in section III. The superiority of the optimized scheme in improving the test efficiency is proved. Section IV concludes the paper.

II. BACKGROUND THEORY

This section presents the theory of antenna pattern reconstruction based on a small number of initial sampling points. Firstly, the theory of spherical wave expansion is described. Then, the clustering method is introduced to divide the initial sampling points into several subclasses, and the calculation process of introducing new sampling data by using the GP optimization algorithm is given. Finally, the near-field data is reconstructed to obtain the antenna pattern. The detailed measurement process is as follows.

According to the uniqueness theorem and the equivalence principle, the radiation field in the outer space of the closed surface can be calculated and determined through the tangential component of the electromagnetic field on the closed surface including all the radiation sources. In the SNFT, an equivalent spherical surface is used to completely surround the AUT, and a passive region is established outside the spherical surface, as shown in Fig. 1.

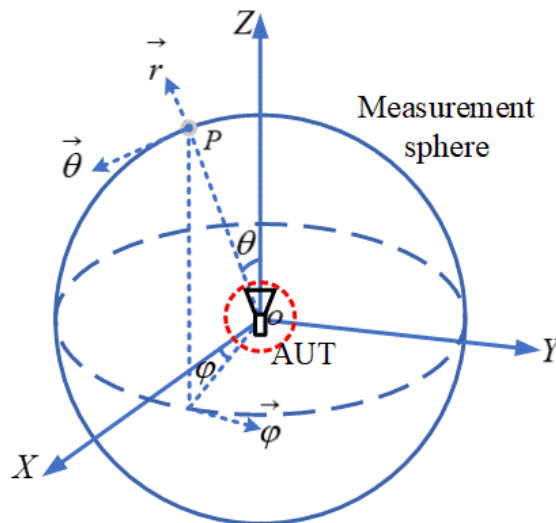


Fig. 1. Schematic of SNFT.

Outside the minimum sphere of the AUT, the electric field can expand as a weighted sum of spherical wave functions expressed as:

$$E(r, \theta, \varphi) = \sum_{s=1}^2 \sum_{n=1}^N \sum_{m=-n}^n Q_{smn} \vec{F}_{smn}^{(3)}(r, \theta, \varphi), \quad (1)$$

where (r, θ, φ) are the spherical coordinates, Q_{smn} are the SWCs of the AUT, $\vec{F}_{smn}^{(3)}$ are the spherical wave expansion functions, $s = 1$ and 2 represent transverse electric (TE) and transverse magnetic (TM) wave modes, respectively, and m, n are the number of modes of AUT. N is a truncation number for the spherical wave expansion empirically obtained from $N = [kr_0] + 10$,

where k is the wave number, r_0 is the radius of the minimum sphere surrounding the antenna and the square brackets indicate the largest integer smaller than or equal to kr_0 . In equation (1), the spherical wave expansion functions are known, the SWCs Q_{smn} can be solved and the field value at any distance can be obtained.

In order to obtain the dynamic change of the electric field data in the near field of the antenna, $M_{initial}$ sampling data are randomly selected from the uniform spherical near field sampling dataset S_2 as the initial samples set as S_1 . The K-means clustering method is used to cluster the $M_{initial}$ sampled data into k subclasses, and each subclass randomly selects a sample as the cluster center. Minkowski distance ($p = 2$ means Euclidean distance) is used to measure the deviation of each sample value from the cluster center and each sample is classified into the subclass where the cluster center with the closest distance is located. The cluster center of each subclass is updated to the average value of all points in the subclass, and the samples are reclassified until the cluster center of all subclasses no longer changes or the total clustering error in all subclasses is the smallest. The current total clustering error in all subclasses is:

$$d = \left(\sum_{j=1}^k \sum_{x_i \in C_j, c_j \in C_j} |x_i - c_j|^p \right)^{\frac{1}{p}}, \quad (2)$$

where x_i is the i -th sample and c_j is the cluster center belonging to the j -th subclass C_j .

After obtaining the cluster classification results, the initial near-field sampling data is sorted according to the sample sampling density and the rate of variation of adjacent samples, and the top ranking represents the area that needs to be interpolated. In order to calculate the sampling density, the initial sampling points are represented by a Voronoi diagram according to the nearest neighbor principle [27]. Each initial sampling point corresponds to a cell, and the sampling density is determined by the area of each cell. Each sampling point is associated with its nearest neighbor cell, and the sample variation rate is expressed as the gradient of the field between adjacent sampling points. So the overall evaluation parameter can be expressed as:

$$G(x_m) = \alpha \left(1 + \frac{S(x_m)}{\sum_{p=1}^{M_{initial}} S(x_p)} \right) + \beta \left(1 + \frac{V(x_m)}{\sum_{p=1}^{M_{initial}} V(x_p)} \right), \quad (3)$$

where $S(x_m)$ is the area of the m th cell, $V(x_m)$ is the sum of the absolute values of all gradients around the m th cell and α, β (satisfying $\alpha + \beta = 1$) are the weighting coefficients. α and β are adjusted accordingly according to the cluster classification results. If the sampling variation rate in a subclass is too large, in order to better judge the interpolation requirements of the sampling area, it is necessary to increase the proportion of sampling density

in the overall evaluation parameters, that is, increase the value of α .

According to the judgment criteria, part of the data to be interpolated comes from the dataset S_2 , and a small amount of data that is not located in the dataset S_2 with uniform sampling interval. A modified Akima piecewise cubic Hermite interpolation method is used in this part.

In order to reduce the truncation error caused by the near-far field conversion after zero-filling the non-essential interpolation area with smooth dynamic changes, the GP algorithm is introduced to extrapolate the sampled values. It is a band-limited extrapolation algorithm that extrapolates the data outside the interval from the known interval, and it is iteratively implemented by using Fourier transform and inverse Fourier transform. Plane wave spectra (PWS) of spherical near-field probe sampled data is obtained from truncated NF measurements using Fourier transforms:

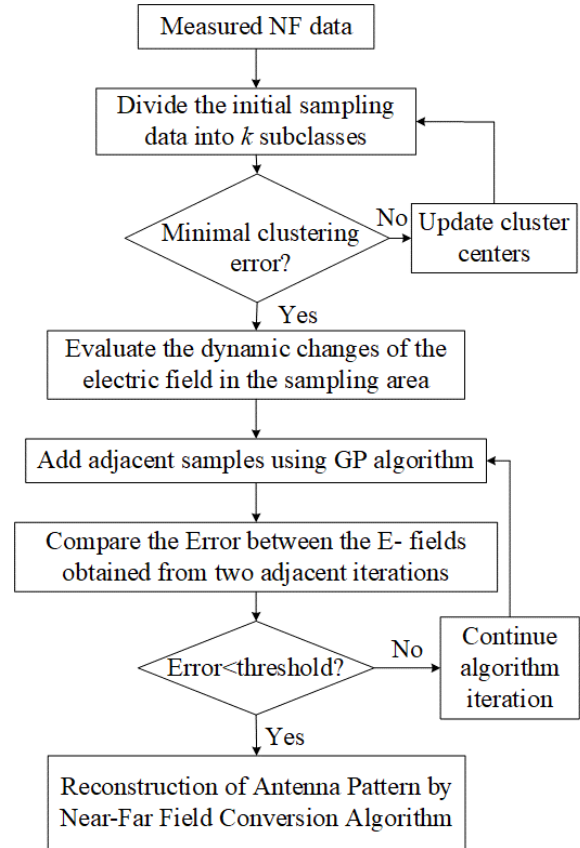


Fig. 2. Schematic diagram of the proposed method.

$$G_0(\theta_k, \varphi_k) = fft[g_0(\theta_k, \varphi_k)], \quad (4)$$

where $g_0(\theta_k, \varphi_k)$ is the cluster-interpolated accessible near field data. The filter functions in the spectral and space domain are:

$$H_R(\theta_k, \varphi_k) = \begin{cases} 1, & (\theta_k, \varphi_k) \in \Omega_0 \\ 0, & (\theta_k, \varphi_k) \notin \Omega_0 \end{cases}, \quad (5)$$

and

$$h(\theta_k, \varphi_k) = \begin{cases} 1, & (\theta_k, \varphi_k) \in \omega_0 \\ 0, & (\theta_k, \varphi_k) \notin \omega_0 \end{cases}, \quad (6)$$

where ω_0 and Ω_0 are reliable regions of the space and spectrum. The electric field on the sampling surface obtained by extrapolation is given by the following equation:

$$\begin{aligned} \xi_{n+1}(\theta_k, \varphi_k) &= \hat{\xi}_n(\theta_k, \varphi_k) + (g_0(\theta_k, \varphi_k) \\ &\quad - \hat{\xi}_n(\theta_k, \varphi_k))h(\theta_k, \varphi_k), \end{aligned} \quad (7)$$

where

$$\hat{\xi}_{n+1}(\theta_k, \varphi_k) = \text{ifft}[\text{fft}[H_R(\theta_k, \varphi_k)G_n(\theta_k, \varphi_k)]]. \quad (8)$$

The PWS of the reliable region is:

$$G_n(\theta_k, \varphi_k) = \text{fft}[g_n(\theta_k, \varphi_k)], \quad (9)$$

where fft and ifft means Fourier transform and inverse Fourier transform, n is the value of iteration times, (θ_k, φ_k) is the k th sampling point on the spherical grid and $g_n(\theta_k, \varphi_k)$ is the optimization extrapolation result for the n th iteration. The error of the near-field data obtained from two adjacent iterations is expressed as

$$\text{Error} = \sum_{k=1}^{M_{\text{total}}} |g_{n+1}(\theta_k, \varphi_k) - g_n(\theta_k, \varphi_k)|^2, \quad (10)$$

where M_{total} is the total effective NF data after extrapolation. After several iterations, the error reaches a stable convergence point and the iteration terminates.

A schematic diagram of the proposed method is shown in Fig. 2, where a small amount of sampling data is used to verify the effectiveness of the clustering technique and the GP extrapolation algorithm to estimate the electric field in the extended area.

III. MEASUREMENT RESULTS

A commercial antenna operating at 2.6 GHz, which is invisible internally, was tested in the spherical near-field multi-probe anechoic chamber of the China Academy of Information and Communications Technology (CAICT). The radius of the SNFT system is 1.6 m, and the minimum spherical radius surrounding the antenna is 0.156 m, as shown in Fig. 3. Figure 4 shows the antenna pattern obtained by using commercial software to calculate the NF data, which is set as the reference radiation pattern.

In order to obtain the initial small amount of sampling data, the NF sampling interval is set to 15 degrees and there is a truncation in the range from $\theta = 165^\circ$ to $\theta = 180^\circ$ degrees due to the influence of the south pole. To improve the test accuracy, triple uniform oversampling ($\Delta\theta = \Delta\varphi = 5^\circ$) is necessary. The uniformly sampled dataset and triple oversampled dataset are set as S_1 and S_0 respectively, and 150 sampling points are selected from S_1 as the initial data set S_2 .

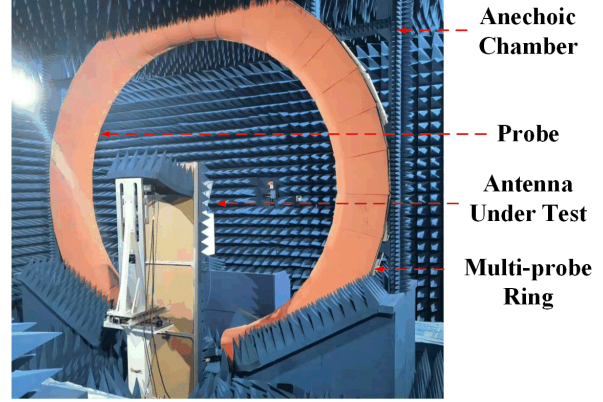


Fig. 3. The spherical NF measurement environment.

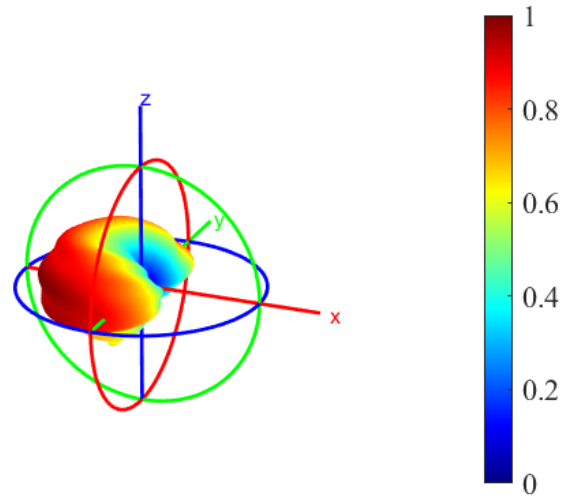


Fig. 4. Reference radiation pattern at 2.6 GHz.

The K-means clustering method divides the sampled values into k subclasses, and for each k value, the sum of the squared distances from every sample to the nearest cluster center is calculated as the total clustering error. As shown in Fig. 5 (a), the total cluster error converges to a stable value at $k = 6$ and Fig. 5 (b) shows the cluster classification results for $k = 6$. Figure 6 shows the Voronoi diagram cell classification results for the initial sampling of the NF. Using equation (3), the area of each cell and the variation rate of adjacent sampling points are calculated. The cell groups whose base sites are red represent highly dynamic areas requiring interpolation, and blue areas represent unnecessary interpolation region.

We use the interpolation method mentioned in the previous section to obtain the dataset S_3 with truncated regions. Dataset S_4 is extrapolated from dataset S_3 by GP algorithm. Figure 7 (a) shows the error of two adjacent iterations of the co-polarization (CP) and

cross-polarization (XP) of the antenna. When the GP algorithm iterates 80 times, the error converges. Figure 7 (b) shows the normalized iterative error of the oversampled electric field and the electric field obtained by the proposed method.

Figure 8 (a) shows the radiation pattern reconstructed from the dataset S_4 . Figure 8 (b) shows the relative

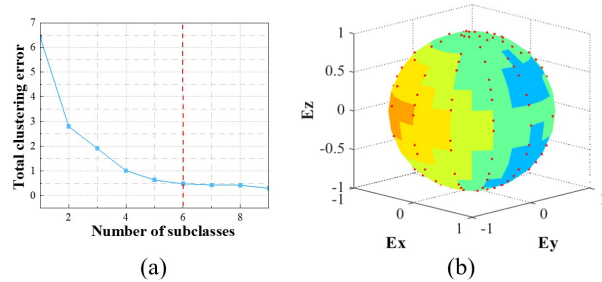


Fig. 5. K-means clustering method. (a) L-curve. (b) Clustering method, $k = 6$.

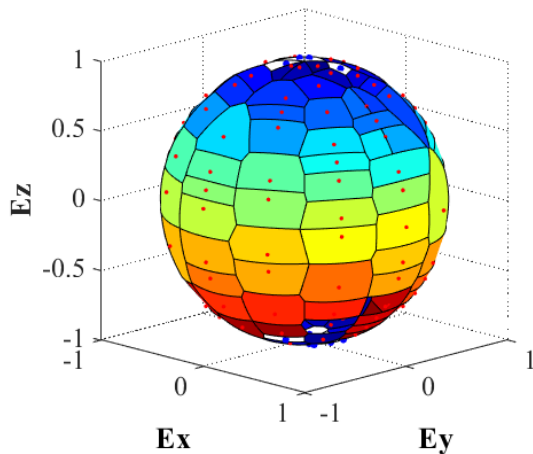


Fig. 6. Voronoi diagram classification for near-field sampling.

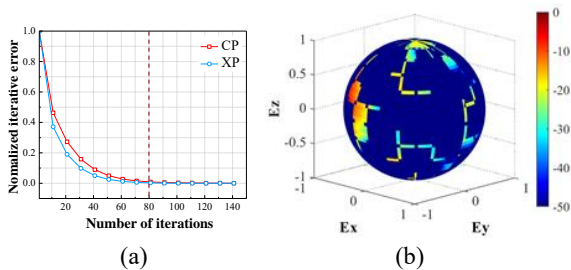


Fig. 7. (a) The normalized iterative error of CP and XP components obtained from two adjacent iterations. (b) Relative error of S_4 and S_0 in all angles.

ative error of reference and reconstructed radiation pattern. The relative error can be obtained using:

$$\text{Relative Error} = 20 \log \left| \frac{|E_1|}{|E_2|} \right|, \quad (11)$$

where E_1 and E_2 are the two electric fields to be compared, respectively. Comparisons of CP and XP components in XOY plane and XOZ plane between reference pattern, the pattern reconstructed by triple oversampling and optimal sampling by the proposed algorithm are given in Fig. 9. As can be seen, the main lobe of

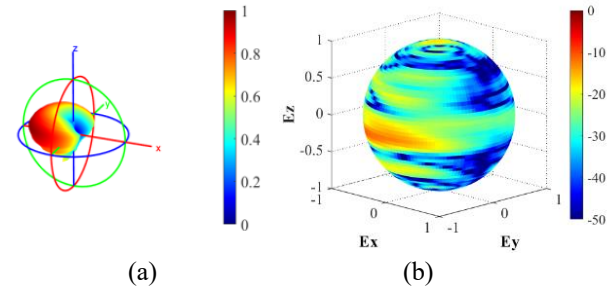


Fig. 8. (a) Reconstructed radiation pattern. (b) Relative error of reference and reconstructed radiation pattern in all angles.

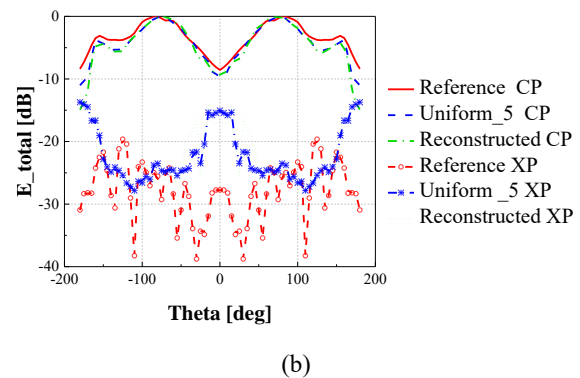
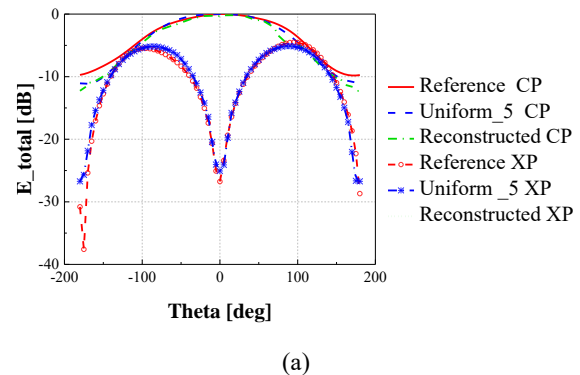
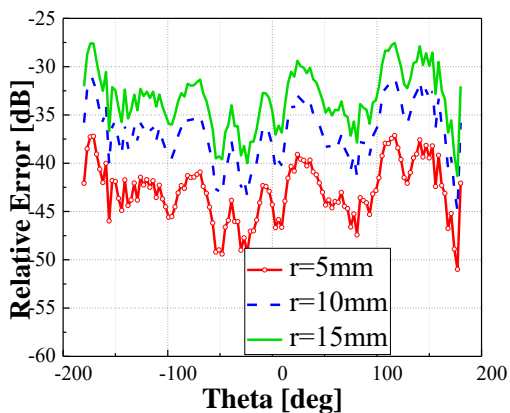


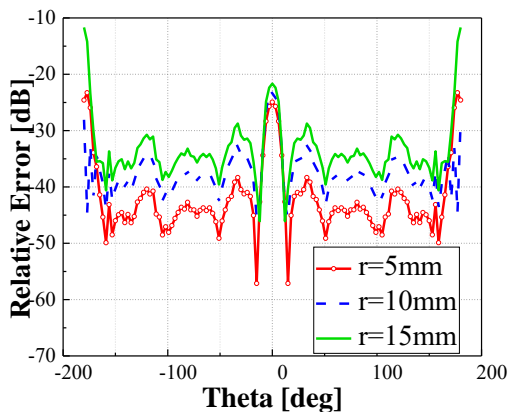
Fig. 9. Comparisons of CP and XP components in (a) XOY plane, and (b) XOZ plane between reference pattern, pattern reconstructed by triple oversampling and optimal sampling by the proposed algorithm.

the CP component of the pattern is in good agreement, but the reconstruction result of the XP has a large error compared with the reference pattern, especially in XOZ plane.

It is noted that the possible positioning error in the actual test affects the pattern recovery. Figures 10 and 11 show the interference errors in XOY plane and XOZ plane introduced when the radial errors are 5 mm, 10 mm and 15 mm, respectively, and the θ angle errors are 0.01 deg, 0.5 deg and 1 deg, respectively. The radial position error in spherical NF scanning mainly affects the phase error in the near field, which is proportional to the radial error. The θ angle error between the actual and the ideal alignment direction of the AUT makes the maximum gain direction of the probe antenna deviate from the center of the SNFT system, which changes the test distance and causes the change of the probe receiving strength to affect the recovery of the pattern.

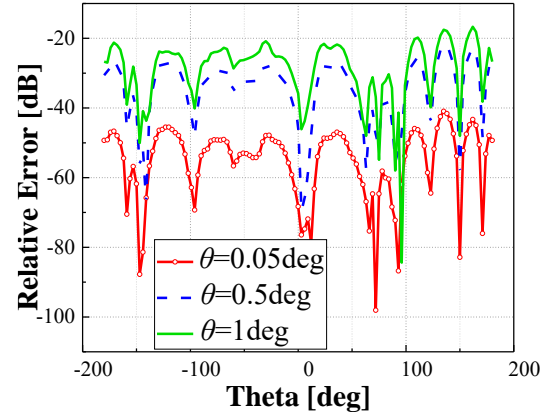


(a)

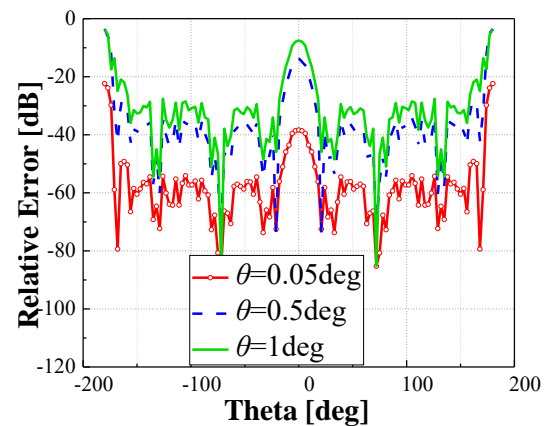


(b)

Fig. 10. The relative errors in (a) XOY plane, and (b) XOZ plane introduced when the radial errors are 5 mm, 10 mm, and 15 mm, respectively.



(a)



(b)

Fig. 11. The relative errors in (a) XOY plane, (b) XOZ plane introduced when the θ angle errors are 0.01 deg, 0.5 deg, and 1 deg, respectively.

IV. CONCLUSION

This paper proposes a method to improve the sampling efficiency of spherical near-field testing. Starting from a small number of near-field sampling points, the region with high dynamic variation of the electric field is located through the clustering classification theory for appropriate interpolation. The GP algorithm is used to extrapolate the unnecessary interpolation area to further improve the sampling accuracy and reduce the truncation error. The multi-probe spherical near-field anechoic chamber test was carried out on a commercial antenna working at 2.6 GHz. The feasibility of this scheme is demonstrated by comparing the reference radiation pattern with the radiation pattern reconstructed by three oversampling and optimized samplings. The influence of the test positioning error on the reconstructed pattern is further discussed.

REFERENCES

- [1] J. E. Hansen, *Spherical Near-Field Antenna Measurements*, Peter Peregrinus, London, UK, 1988.
- [2] T. M. Gemmer and D. Heberling, "Accurate and efficient computation of antenna measurements via spherical wave expansion," *IEEE Trans. Antennas Propag.*, vol. 68, no. 12, pp. 8266-8269, Dec. 2020.
- [3] T. B. Hansen, "Spherical near-field scanning with higher-order probes," *IEEE Trans. Antennas Propag.*, vol. 59, no. 11, pp. 4049-4059, Nov. 2011.
- [4] T. Laitinen, S. Pivnenko, J. M. Nielsen, and O. Breinbjerg, "Theory and practice of the FFT/matrix inversion technique for probe-corrected spherical near-field antenna measurements with high-order probes," *IEEE Trans. Antennas Propag.*, vol. 58, no. 8, pp. 2623-2631, Aug. 2010.
- [5] R. Cornelius and D. Heberling, "Spherical near-field scanning with pointwise probe correction," *IEEE Trans. Antennas Propag.*, vol. 65, no. 2, pp. 995-997, Feb. 2017.
- [6] L. Zhiping, Z. Wang, and W. Jianhua, "Computer reconstructed holographic technique for phase-less near-field measurement," *Applied Computational Electromagnetics Society (ACES) Journal*, vol. 28, no. 12, pp. 1199-1204, Sep. 2021.
- [7] F. S. de Adana, O. Gutiérrez, L. Lozano, and M. Cátedra, "A new iterative method to compute the higher order contributions to the scattered field by complex structures," *Applied Computational Electromagnetics Society (ACES) Journal*, vol. 21, no. 2, pp. 115-126, Jun. 2022.
- [8] J. Zheng, X. Chen, X. Liu, M. Zhang, B. Liu, and Y. Huang, "An improved method for reconstructing antenna radiation pattern in a loaded reverberation chamber," *IEEE Trans. Instrum. Meas.*, vol. 71, Art. no. 8001812, 2022.
- [9] Q. Xu, Y. Huang, L. Xing, C. Song, Z. Tian, S. S. Alja'afreh, and M. Stanley, "3-D antenna radiation pattern reconstruction in a reverberation chamber using spherical wave decomposition," *IEEE Trans. Antennas Propag.*, vol. 65, no. 4, pp. 1728-1739, Apr. 2017.
- [10] R. R. Alavi and R. Mirzavand, "Range extension in partial spherical near-field measurement using machine learning algorithm," *IEEE Antennas Wireless Propag. Lett.*, vol. 19, no. 11, pp. 2003-2007, Nov. 2020.
- [11] X. Li, T. Zhang, M. Wei, and L. Yang, "Reduction of truncation errors in planar near-field antenna measurements using improved Gerchberg-Papoulis algorithm," *IEEE Trans. Instrum. Meas.*, vol. 69, no. 9, pp. 5972-5974, Sept. 2020.
- [12] K. T. Kim, "Truncation-error reduction in spherical near-field scanning using Slepian sequences: Formulation for scalar waves," *IEEE Trans. Antennas Propag.*, vol. 59, no. 8, pp. 2813-2823, Aug. 2011.
- [13] F. J. Cano-Facila, S. Pivnenko, and M. Sierra-Castañer, "Reduction of truncation errors in planar, cylindrical, and partial spherical near-field antenna measurements," *Int. J. Antennas Propag.*, pp. 186-187, 2012.
- [14] O. M. Bucci and M. D. Migliore, "A new method for avoiding the truncation error on near-field antenna measurements," *IEEE Trans. Antennas Propag.*, vol. 54, no. 10, pp. 2940-2952, Oct. 2006.
- [15] E. Martini, O. Breinbjerg, and S. Maci, "Reduction of truncation errors in planar near-field aperture antenna measurements using the Gerchberg-Papoulis algorithm," *IEEE Trans. Antennas Propag.*, vol. 56, no. 11, pp. 3485-3493, Nov. 2008.
- [16] O. M. Bucci and M. D. Migliore, "A new method for avoiding the truncation error on near-field antenna measurements," *IEEE Trans. Antennas Propag.*, vol. 54, no. 10, pp. 2940-2952, Oct. 2006.
- [17] F. D'Agostino, F. Ferrara, C. Gennarelli, G. Gennarelli, R. Guerriero, and M. Migliozzi, "On the direct non-redundant near-field-to-far-field transformation in a cylindrical scanning geometry," *IEEE Antennas Propag. Mag.*, vol. 54, no. 1, pp. 130-138, Feb. 2012.
- [18] F. D'Agostino, F. Ferrara, C. Gennarelli, R. Guerriero, and M. Migliozzi, "Non-redundant spherical NF-FF transformations using ellipsoidal antenna modeling: Experimental assessments [measurements corner]," *IEEE Antennas Propag. Mag.*, vol. 55, no. 4, pp. 166-175, Aug. 2013.
- [19] B. Hofmann, O. Neitz, and T. F. Eibert, "On the minimum number of samples for sparse recovery in spherical antenna near-field measurements," *IEEE Trans. Antennas Propag.*, vol. 67, no. 12, pp. 7597-7610, Dec. 2019.
- [20] C. Culotta-López and D. Heberling, "Adaptive sampling for compressed spherical near-field measurements," *Antenna Measurement Techniques Association Symposium (AMTA)*, Newport, RI, pp. 1-6, 2020.
- [21] F. R. Varela, B. G. Iragüen, and M. Sierra-Castañer, "Application of nonuniform FFT to spherical near-field antenna measurements," *IEEE Trans. Antennas Propag.*, vol. 68, no. 11, pp. 7571-7579, Nov. 2020.
- [22] F. R. Varela, B. G. Iragüen, and M. Sierra-Castañer, "Near-field to far-field transformation on arbitrary surfaces via multi-level spherical wave expansion," *IEEE Trans. Antennas Propag.*, vol. 68, no. 1, pp. 500-508, Jan. 2020.
- [23] R. R. Alavi, R. Mirzavand, J. Doucette, and P. Mousavi, "An adaptive data acquisition and clus-

tering technique to enhance the speed of spherical near-field antenna measurements,” *IEEE Antennas Wireless Propag. Lett.*, vol. 18, no. 11, pp. 2325-2329, Nov. 2019.

- [24] Y. Wang, T. F. Eibert, and Z. Nie, “Adaptive cross approximation algorithm accelerated inverse equivalent current method for near-field antenna measurement,” *IEEE Trans. Antennas Propag.*, vol. 67, no. 3, pp. 1874-1883, Mar. 2019.
- [25] R. R. Alavi, R. Mirzavand, and P. Mousavi, “Fast and accurate near-field to far-field transformation using an adaptive sampling algorithm and machine learning,” *IEEE International Symposium on Antennas and Propagation and USNC-URSI Radio Science Meeting*, Atlanta, GA, pp. 225-226, 2019.
- [26] T. F. Eibert, E. Kılıç, C. Lopez, R. A. Mauermayer, O. Neitz, and G. Schnattinger, “Electromagnetic field transformations for measurements and simulations (invited paper),” *Prog. Electromagn. Res.*, vol. 151, pp. 127-150, May 2015.
- [27] J. Zheng, X. Chen, and Y. Huang, “An effective antenna pattern reconstruction method for planar near-field measurement system,” *IEEE Trans. Instrum. Meas.*, vol. 71, Art. no. 8005012, Jul. 2022.



Fangyun Peng received her B.Sc. degree in Electrical Information Engineering from Southwest Jiaotong University, Chengdu, China, in 2018. She is currently pursuing a Ph.D. degree at the School of Electronic and Information Engineering from Xi’an Jiaotong University. Her research interests include over-the-air testing.



Yuchen Ma was born in Beijing, China, in 1993. He received his B.E. degree and doctorate from the School of Electronic and Information Engineering, Beijing Jiaotong University, Beijing, China, in 2015 and 2021, respectively. He is currently at the China Academy of Information and Communications Technology, Beijing, China. His current research interests include near-field measurement and antenna design.



Yuxin Ren received his M.Sc. degree in Electronic Science and Technology from the Beijing University of Posts and Telecommunications, Beijing, in 2014. Since 2018, he has been an engineer at the China Academy of Information and Communications and Technology. His current research interests include the theory of reverberation chambers, plane wave synthesizers, and other OTA test systems.

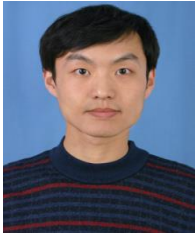


Bo Liu received his B.Sc. degree in Electronic Information Engineering from Xidian University, Xi’an, China, in 2019. He received his M.Sc. degree from the School of Electronic and Information Engineering, Xi’an Jiaotong University, Xi’an, China, in 2022. His research interests include MIMO antennas and the decoupling of MIMO antennas.



Xiaobo Liu (Member, IEEE) was born in Baoji, China, in 1992. He received his B.Eng. degree in Information Engineering and his Ph.D. degree in Electronic Science and Technology from Xi’an Jiaotong University, Xi’an, China, in 2014 and 2018, respectively. From 2018 to 2020, he was a Research Associate with Xi’an Jiaotong University. Since 2020, he has been a Post-Doctoral Fellow in Applied Mathematics and an Assistant Professor with Xi’an Jiaotong University. He has authored or coauthored more than 20 articles in international and domestic journals and conferences. His research interests include electromagnetic and microwave theory, computational electromagnetics, metasurface, antenna design, and microwave circuit.

Dr. Liu serves as a reviewer for the following IEEE journals: *IEEE Transactions on Microwave Theory and Techniques* (TMTT), the *IEEE Microwave and Wireless Components Letters* (MWCL), and the *IEEE Antennas and Wireless Propagation Letters* (AWPL).



Zhengpeng Wang (M'15) was born in Shandong, China, in 1981. He received his B.Sc. degree in Electronic Science and Technology from Shandong University, Jinan, China, in 2004, and his M.Sc. and Ph.D. degrees in Electromagnetic Field and Microwave Technology from Beihang University, Beijing, China, in 2007 and 2012, respectively.

He was a Visiting Researcher with the Antenna and Applied Electromagnetic Laboratory, University of Birmingham, Birmingham, U.K., in 2009 and 2010. From 2013 to 2015, he was a Research Fellow with the University of Kent, Canterbury, U.K., and the University of Science and Technology Beijing, Beijing, China. He is currently an Associate Professor at Beihang University. His current research interests include over-the-air (OTA) testing, reconfigurable antennas, compact antenna test range feed antenna and antenna measurement.



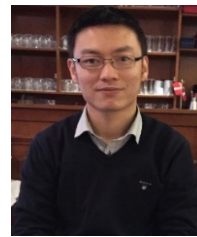
Lei Zhao (Senior Member, IEEE), received his B.S. degree in Mathematics from Jiangsu Normal University, China, in 1997. He received his M.S. degree in Computational Mathematics and Ph.D. degree in Electromagnetic Fields and Microwave Technology, both from Southeast

University, Nanjing, China, in 2004 and 2007, respectively.

He joined the China University of Mining and Technology, Xuzhou, China, in 2019, where he is currently a Full Professor. From September 2009 to December 2018, he worked at Jiangsu Normal University, Xuzhou, China. From August 2007 to August 2009, he worked at the Department of Electronic Engineering, The Chinese University of Hong Kong, as a Research Associate. From February 2011 to April 2011, he worked at the Department of Electrical and Computer Engineering, National University of Singapore, as a Research Fellow. From September 2016 to September 2017, he worked at the Department of Electrical and Computer Engineering, University of Illinois at Urbana-Champaign, Champaign, IL, USA, as a Visiting Scholar. He has authored or coauthored more than 90 refereed journal and conference papers. His current research interests include spoof surface plasmon polaritons theory and its applications, RF/microwave antenna and filter design, computational electromagnetics, and electromagnetic radiation on the human body.

Dr. Zhao serves as an Associate Editor for *IEEE Access*, an Associate Editor-in-Chief and reviewer for

the *Applied Computational Electromagnetics Society (ACES) Journal* and is a reviewer for multiple journals and conferences including *IEEE Trans. on Microwave Theory and Techniques*, *IEEE Trans. Antennas and Propagation*, *IEEE Antennas and Wireless Propagation Letters*, and other primary electromagnetics and microwave-related journals.



Xiaoming Chen received his B.Sc. degree in Electrical Engineering from Northwestern Polytechnical University, Xi'an, China, in 2006, and M.Sc. and Ph.D. degrees in Electrical Engineering from Chalmers University of Technology, Gothenburg, Sweden, in 2007 and

2012, respectively. From 2013 to 2014, he was a post-doctoral researcher at that same university. From 2014 to 2017, he was with Qamcom Research & Technology AB, Gothenburg, Sweden. Since 2017, he has been a professor at Xi'an Jiaotong University, Xi'an, China. His research areas include MIMO antennas, over-the-air testing and reverberation chambers, and has published more than 150 journal articles on these topics.

Prof. Chen currently serves as a Senior Associate Editor for *IEEE Antennas and Wireless Propagation Letters*. He was the general chair of the *IEEE International Conference on Electronic Information and Communication Technology (ICEICT)* in 2021. He won first prize for the universities' scientific research results in Shaanxi province, China, 2022. He received the IEEE outstanding Associate Editor awards in 2018, 2019, 2020, 2021, and the URSI (International Union of Radio Science) Young Scientist Award in 2017 and 2018.



Zhiqin Wang is the vice president of the China Academy of Information and Communications Technology. She is the chair of the CCSA Wireless Technical Committee. She is dedicated to pioneering research and practice in the field of mobile communications, and has specialized in mobile communications' technical research and standards. She is the chair of IMT-2020 (5G) Promotion Group in China and the vice chief engineer of the major project "New Generation Broadband Wireless Mobile Telecommunications".